

Stability and self-stabilisation of single-frequency lasing in a semiconductor laser

D.V. Batrak, A.P. Bogatov, F.F. Kamenets

Abstract. The problem of stability of single-frequency lasing is considered using a model including one lasing mode and two nearest subthreshold modes. It is shown that, the parametric interaction of the laser and subthreshold modes, due to the electron concentration beats at the intermode frequency, can cause the self-stabilisation of the single-frequency lasing regime, in which the laser frequency detuning with respect to the spectral gain maximum can exceed the mode interval, and spectral hysteresis can be observed.

Keywords: semiconductor laser, single-frequency lasing, nonlinear mode interaction, self-stabilisation, frequency tuning.

1. Introduction

The emission spectrum of a semiconductor laser is one of its main characteristics determining to a great extent the possibilities of applications of the laser. The emission spectrum may contain a few excited longitudinal modes whose number depends on the laser resonator design. As a rule, this is explained by the fact that the spectral gain band is many times broader than the mode interval. However, because of the quasi-homogeneous broadening of the gain line of a semiconductor [1–3], a strong competition occurs between different spectral emission components representing different longitudinal modes. This competition favours single-frequency lasing at one longitudinal mode of the resonator.

Along with the above-mentioned factors, the emission spectrum of a laser depends on the optical nonlinearity of the laser medium caused by the saturation effect. This mechanism is fundamental for all lasers. A consideration of this nonlinearity leads to the relation between the amplitudes of fields at different frequencies, which has been studied already in early papers on gas and solid-state lasers [4–6]. As for semiconductor lasers, this optical nonlinearity has a specific feature, which is manifested as oscillations in the carrier concentration caused by the total

emission intensity beats at the intermode frequency. This mechanism was first considered in paper [7] and then was used to describe the interaction between the waves (see Refs [8–13] and references therein).

The results obtained in these earlier papers explained the behaviour of a semiconductor laser with an external resonator in which the intensity beat frequency was not much higher than the inverse interband relaxation time of carriers. However, attempts to interpret experimental data on the formation of the emission spectrum in a laser with a resonator formed by crystal facets (intrinsic resonator) encountered certain difficulties because of the unsatisfactory reproducibility and ambiguity of the data.

In the case of a laser with an intrinsic resonator, the efficiency of interaction between the modes through inversion beats decreases by more than two orders of magnitude compared to the case of an external resonator. It is by this factor that the intermode beat frequency exceeds the inverse interband relaxation time. However, the fact itself that the beat frequency is much higher than the inverse relaxation time does not mean that this mechanism is insignificant in the formation of the emission spectrum. The induced nonlinear gain should be compared with the gain deficit for subthreshold modes. We will show below that these quantities are comparable already at a moderate intensity of lasing. Therefore, this mechanism remains one of the basic mechanisms in the case of lasers with an intrinsic resonator as well.

The difficulties encountered in the interpretation of experimental data are probably caused by small absolute gain deficits for subthreshold modes, resulting in a significant role of another factor, namely, a random spectral selectivity of the resonator. It is well known [14–17] that the presence of an optical inhomogeneity along the resonator axis results in the modulation of the envelope of the effective amplification for longitudinal modes. Because this modulation depends on the position of inhomogeneities and their amplitude, which are random, this modulation of the spectral curve is also random. It can provide the preferable lasing at some mode if the gain for this mode increases. In this way, a random selectivity of the resonator emerges. The gain deficiencies for subthreshold modes nearest to the lasing mode also become random quantities. Their values can strongly differ for different samples.

Advances in the modern technology of fabrication of heterolasers allow us to hope that the number of technological imperfections of modern semiconductor lasers is small enough for the random selectivity of the laser resonator not to be its dominating property. In this

D.V. Batrak, F.F. Kamenets Moscow Institute of Physics and Technology (State University), Institutskii per. 9, 141700 Dolgoprudnyi, Moscow region, Russia;

A.P. Bogatov P.N. Lebedev Physics Institute, Russian Academy of Sciences, Leninskii prosp. 53, 119991 Moscow, Russia

Received 15 January 2003

Kvantovaya Elektronika 33 (11) 941–948 (2003)

Translated by M.N. Sapozhnikov

connection, it is important at present to analyse the stability of the single-frequency regime of a semiconductor laser in a model including fundamental physical mechanisms, in particular, the gain saturation and dynamic inversion oscillations caused by intensity beats. The presence of such oscillations is a fundamental property of the laser system. Such studies are also urgent because of practical applications of tunable single-frequency lasers, for example, in optical communications and laser spectroscopy. Although analysis performed in this paper has a general character, it nevertheless first of all can be applied to InGaAs/AlGaAs/GaAs and InGaAsP/AlInGaAsP/InP heterolasers emitting in the visible and IR spectral regions and having the best emission properties.

2. System of equations for coupled modes

Within the framework of a semiclassical approach, which we will use in the paper, the interaction of a semiconductor active medium with an electromagnetic field is described in terms of the permittivity. We assume that the field in the laser satisfies the scalar wave equation written in the form

$$\nabla^2 E(\mathbf{r}, t) - \frac{1}{c^2} \frac{\partial^2}{\partial t^2} [\hat{\varepsilon} E(\mathbf{r}, t)] = 0, \quad (1)$$

where $\hat{\varepsilon} = \hat{\varepsilon}(\mathbf{r})$ is the permittivity operator of the medium.

The solution of this equation corresponding to the single-frequency regime is written in the form

$$E_0(\mathbf{r}, t) = \text{Re} [C_0 e^{-i\omega_0 t} u(x, y) (F_+ e^{i\beta_0 z} + F_- e^{-i\beta_0 z})], \quad (2)$$

$$0 \leq z \leq L,$$

where C_0 is the real quantity characterising the amplitude of the laser-mode field; $u(x, y)$ is the transverse distribution of the field, which is assumed real; β_0 is the complex propagation constant [$u(x, y)$ and β_0 are described in Appendix]; L is the laser diode length; and the z axis is directed along the resonator axis. The constant coefficients F_+ and F_- characterise the relation between amplitudes of the waves propagating in the positive and negative directions along the z axis. Taking into account the boundary conditions at the laser facets, we obtain $F_+/F_- = r_1$. We determine the absolute values of these coefficients by the normalisation condition

$$\frac{1}{V_{\text{ar}}} \int |u(x, y) (F_+ e^{i\beta_0 z} + F_- e^{-i\beta_0 z})|^2 dV = 1$$

(integration is performed over the volume V_{ar} of the active region).

The boundary conditions for $z = 0, L$ lead to the following expressions for the real and imaginary parts of β_0 :

$$\beta_0' = \frac{\pi k}{L} - \frac{\arg(r_1 r_2)}{2L}, \quad (3)$$

$$\beta_0'' = \frac{1}{2L} \ln |r_1 r_2|, \quad (4)$$

where r_1, r_2 are the amplitude reflection coefficients of the laser facets and k is a natural number. Equation (3)

determines the mode frequencies of the resonator, while equation (4) is the condition of the equality of the gain and losses.

Let us analyse the stability of lasing at a given mode. For this purpose, we will study the response of our system to the appearance of small additions to the field at other modes (for example, due to spontaneous emission). In single-frequency lasers, all the transverse modes, except the lasing mode, are usually strongly suppressed. Therefore, we will consider only longitudinal modes. The transverse structure of the field in this case weakly depends on the mode number (and the pump level), and its variations can be neglected here by representing the field in the laser in the form

$$E(\mathbf{r}, t) = \text{Re} \left[u(x, y) \sum_m C_m(t) e^{-i\omega_m t} V_m(z) \right], \quad (5)$$

where $C_m(t)$ is the slow complex amplitude of the m th mode field and $V_m(z)$ is the longitudinal distribution of the m th mode field. We will read the mode number m from the lasing mode, for which we assume that $C_0(t) = C_0 = \text{const}$. The value of C_0 is assumed real (which can be always obtained by a proper choice of the time reading). We also assume that $|C_m(t)| \ll C_0$ for $m \neq 0$, and all the expressions below will be written in the linear approximation in $C_m(t)$.

The interference of the fields of the laser and side modes leads to the appearance of the radiation intensity beats at frequencies that are multiples to the mode interval

$$\overline{E^2} \approx \frac{1}{2} [u(x, y)]^2 \left\{ C_0^2 |V_0(z)|^2 + \sum_{m \neq 0} [C_0 C_m^* V_0(z) V_m^*(z) e^{i(\omega_m - \omega_0)t} + \text{c.c.}] \right\}. \quad (6)$$

As a result, due to the saturation effect, a variable addition $\delta N(\mathbf{r}, t)$ appears to the carrier concentration in the active laser region and the corresponding addition to the complex permittivity

$$\delta \varepsilon(\mathbf{r}, t) = \frac{d\varepsilon}{dN} \delta N(\mathbf{r}, t). \quad (7)$$

The expression for $\delta N(\mathbf{r}, t)$ can be obtained using the balance equation for the carrier concentration

$$\dot{N} + \frac{N}{\tau} - \mu \nabla^2 N + \frac{G(N) c n \overline{E^2}}{4\pi \hbar \omega_0} - J = 0, \quad (8)$$

where τ is the carrier lifetime caused by spontaneous recombination; μ is the diffusion coefficient; $G(N)$ is the material gain of the medium; J is the term describing pump; and the term proportional to $\overline{E^2}$ corresponds to stimulated transitions. Let us represent $N(\mathbf{r}, t)$ and $G(N)$ as a sum of static and dynamic components

$$N(\mathbf{r}, t) = N_0(\mathbf{r}) + \delta N(\mathbf{r}, t), \quad (9)$$

$$G(N) = G(N_0) + \left(\frac{\partial G}{\partial N} \right)_{N=N_0} \delta N(\mathbf{r}, t).$$

By substituting (9) into equation (8) and separating static and dynamic terms, we obtain two equations

$$\frac{N_0}{\tau} - \mu \nabla^2 N_0 + \frac{G(N_0)cn\overline{E_0^2}}{4\pi\hbar\omega_0} - J = 0, \quad (10)$$

$$\begin{aligned} \delta\dot{N} + \frac{\delta N}{\tau_{\text{eff}}(\mathbf{r})} - \mu \nabla^2 \delta N = & -\frac{G(N_0)cn}{8\pi\hbar\omega_0} [u(x, y)]^2 \\ & \times \sum_{m \neq 0} [C_0 C_m^* V_0(z) V_m^*(z) e^{i(\omega_m - \omega_0)t} + \text{c.c.}], \end{aligned} \quad (11)$$

where $\tau_{\text{eff}}(\mathbf{r})$ is the effective lifetime of injected carriers taking into account stimulated transitions

$$\frac{1}{\tau_{\text{eff}}(\mathbf{r})} \equiv \frac{1}{\tau} + \left(\frac{\partial G}{\partial N} \right)_{N=N_0} \frac{cn\overline{E_0^2}}{4\pi\hbar\omega_0}.$$

Equation (10), together with (2) and equations for $u(x, y)$ [see (1) in Appendix] allows us to find the static distribution of the carrier concentration $N_0(\mathbf{r})$ and the amplitude C_0 of the lasing mode. By substituting $N_0(\mathbf{r})$ into (11) and taking into account the slow variation of amplitudes C_m compared to the intermode beat frequency, we can find $\delta N(\mathbf{r}, t)$ in the form

$$\delta N(\mathbf{r}, t) = \sum_{m \neq 0} [f_m(\omega_m - \omega_0, \mathbf{r}) C_0 C_m^* e^{i(\omega_m - \omega_0)t} + \text{c.c.}], \quad (12)$$

where the functions $f_m(\mathbf{r})$ are determined by the equation

$$\begin{aligned} \left[i(\omega_m - \omega_0) + \frac{1}{\tau_{\text{eff}}(\mathbf{r})} - \mu \nabla^2 \right] f_m(\mathbf{r}) = & -\frac{G(N_0)cn}{8\pi\hbar\omega_0} [u(x, y)]^2 \\ & \times V_0(z) V_m^*(z). \end{aligned} \quad (12a)$$

Although the functions $N_0(\mathbf{r})$ and $f_m(\mathbf{r})$ cannot be found analytically in the general case, they can be easily calculated numerically in all practically important cases.

Note that the vector \mathbf{r} in equations (8), (10), and (11) represents only two coordinates: the transverse coordinate y in the $p-n$ junction plane and the longitudinal coordinate z . The dependence of the concentration N on the coordinate x (perpendicular to the structure layers) for modern lasers is described by a piecewise constant function, which is nonzero only within the active layer.

Note also that equation (11) is valid if the beat frequency $\omega_m - \omega_0$ does not exceed the homogeneous width of the gain line of a semiconductor. This is the case when the resonator length L is not too small. For example, when the homogeneous width is ~ 10 meV, the value of L should be $\gtrsim 20$ μm .

The time-oscillating addition $\delta\varepsilon$ to the electric induction produces the field components at the frequencies of the longitudinal modes adjacent to the lasing mode. Therefore, in the presence of a strong field of the lasing mode the interaction appears between these longitudinal modes. By using expressions (12) and (7) and separating components at different frequencies in equation (1) for the field, we can obtain the system of equations for the complex amplitudes of individual modes. This system, in the approximation used here (in the first order in C_m), is decomposed into pairs of equations describing modes that are located at equal distances from the different sides of the lasing mode. As shown in Appendix, these equations can be written in the form ($m > 0$)

$$\begin{aligned} \dot{C}_m(t) + \frac{c}{2\tilde{n}_{\text{gr}}} A_m C_m(t) \\ + (\alpha + i) \frac{c}{2\tilde{n}_{\text{gr}}} \chi_m [A_m C_m(t) + B_m C_{-m}^*(t)] = 0, \\ C_{-m}^*(t) + \left(\frac{c}{2\tilde{n}_{\text{gr}}} A_{-m} + i\kappa_m \right) C_{-m}^*(t) \\ + (-\alpha + i) \frac{c}{2\tilde{n}_{\text{gr}}} \chi_m [A_{-m}^* C_{-m}^*(t) + B_{-m}^* C_m(t)] = 0, \end{aligned} \quad (13)$$

where

$$\chi_m = g_0 \frac{1}{\Omega_m \tau} \frac{I}{I_{\text{sat}}}; \quad \Omega_m \equiv \omega_m - \omega_0 \approx m \frac{\pi c}{\tilde{n}_{\text{gr}} L};$$

A_m and A_{-m} are the gain deficits for the m th and $-m$ th modes; κ_m is the deviation from the equidistant location of the modes (see Fig. 1); \tilde{n}_{gr} is the group modal refractive index; α is the so-called amplitude–phase coupling coefficient (all these parameters are defined in Appendix); $g_0 = L^{-1} \ln(|r_1 r_2|^{-1})$ is the threshold mode gain; $I = cnC_0^2/(8\pi)$ is the lasing mode intensity in the active region; and $I_{\text{sat}} = \hbar\omega_0/[(\partial G/\partial N)\tau]$ is the characteristic intensity of the saturation effect. By using (10), we can show that the value of I/I_{sat} is related to the pump current J by the approximate expression $I/I_{\text{sat}} \approx \eta\theta$, where $\theta = [(N/G)(\partial G/\partial N)]_{N=N_0}$ is a coefficient of the order of unity and $\eta = J/J_{\text{th}} - 1$ is the relative excess of the pump current over its threshold value. The dimensionless complex coefficients A_m and B_m of the order of unity characterise the spatial overlap of the field and the carrier concentration beats and are defined in Appendix.

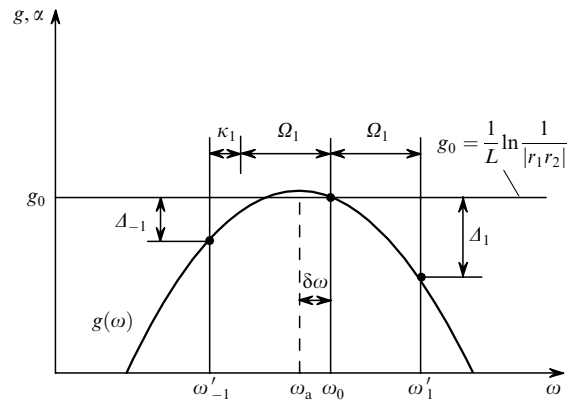


Figure 1. Position of the working point of a laser at the lasing threshold. $g(\omega)$: frequency dependence of the mode gain; ω_0 : lasing frequency; ω_a : maximum gain frequency; $\delta\omega$: lasing frequency detuning from the maximum gain frequency; ω'_1 and ω'_{-1} : frequencies of the subthreshold modes nearest to the lasing frequency in the blue and red regions, respectively; g_0 : threshold gain.

Equations (13) are similar to equations used earlier in Refs [11–13] and describe the amplitudes of coupled oscillations. The coupling between the oscillations [terms proportional to χ_m in system (13)] appeared due to the oscillations of the electron concentration. The frequency of these oscillations can exceed the characteristic time response of the system determined by the value of τ^{-1} by two orders of magnitude and more, however, they cannot be neglected.

As we will show below, the value of χ_m can be of the same order of magnitude as Δ_m , and Δ_{-m} already at moderate radiation intensities.

The general solution of system (13) has the form

$$\begin{pmatrix} C_m(t) \\ C_{-m}^*(t) \end{pmatrix} = Q_m \begin{pmatrix} 1 \\ (\alpha - i)\chi_m B_{-m}^* \\ \zeta_m + \xi_m \end{pmatrix} e^{p_m t} + Q_{-m} \begin{pmatrix} (\alpha + i)\chi_m B_m \\ \zeta_m + \xi_m \\ 1 \end{pmatrix} e^{p_{-m} t}, \quad (14)$$

where $Q_{\pm m}$ are constants; $p_{\pm m} = (c/2\tilde{n}_{\text{gr}})(\eta_m \pm \xi_m)$; and

$$\begin{aligned} \eta_m &= -\frac{1}{2} \left[\Delta_m + \Delta_{-m} + \frac{2i\tilde{n}_{\text{gr}}\kappa_m}{c} + \alpha\chi_m(A_m - A_{-m}^*) \right. \\ &\quad \left. + i\chi_m(A_m + A_{-m}^*) \right]; \\ \zeta_m &= \frac{1}{2} \left[\Delta_{-m} - \Delta_m + \frac{2i\tilde{n}_{\text{gr}}\kappa_m}{c} - \alpha\chi_m(A_m + A_{-m}^*) \right. \\ &\quad \left. + i\chi_m(A_{-m}^* - A_m) \right]; \\ \xi_m &= [(\zeta_m)^2 - (1 + \alpha^2)(\chi_m)^2 B_m B_{-m}^*]^{1/2}. \end{aligned} \quad (15)$$

The sign of the square root in the expression for ξ_m is chosen so that $\text{sign}[\text{Re}(\xi_m)] = \text{sign}(\Delta_{-m} - \Delta_m)$.

Similarly to individual modes, we can introduce for a coupled pair of modes the effective gain deficits

$$\Delta_{\pm m}^{\text{eff}} = -\frac{2\tilde{n}_{\text{gr}}}{c} \text{Re}(p_{\pm m}). \quad (16)$$

Oscillation at the lasing mode will be stable if additions to the field at other modes will decay with time, i.e., when the condition

$$\Delta_{\pm m}^{\text{eff}} > 0 \quad (17)$$

is fulfilled for each pair of the modes. The fulfilment of these conditions can be readily verified by direct calculations by varying the laser system parameters, including the pump current and detuning of the longitudinal resonance of the lasing mode from the spectral maximum of the material gain band.

3. Analysis of the solution

Consider a ridge semiconductor laser with a quantum-well active layer. We will use a simplified model in which the transverse distribution of the field $u(x, y)$ in the active region is described by the expression

$$u(y) \sim \cos \frac{\pi y}{D}, \quad -\frac{D}{2} \leq y \leq \frac{D}{2}, \quad (18)$$

where D is the effective ridge width. We assume that the static electron concentration $N_0(\mathbf{r})$ in the ridge is constant and consider the case of a high- Q resonator ($r_{1,2} \approx 1$). Within the framework of the assumptions made above, the coefficients A_m and B_m are described by the expressions

$$\begin{aligned} A_m &= A_{-m}^* \approx \frac{1}{2} + \frac{1}{4} \left[1 + \frac{i\mu}{\Omega_m} \left(\frac{2\pi}{D} \right)^2 \right]^{-1} \\ &\quad + \frac{3}{4} \left[1 + \frac{i\mu}{\Omega_m} \left(\frac{4\pi\tilde{n}}{\lambda_0} \right)^2 \right]^{-1}, \quad (19) \\ B_m &= B_{-m}^* \approx \frac{1}{2} + \frac{1}{4} \left[1 + \frac{i\mu}{\Omega_m} \left(\frac{2\pi}{D} \right)^2 \right]^{-1}. \end{aligned}$$

Here, λ_0 is the radiation wavelength in vacuum and \tilde{n} is the modal refractive index.

We will find now the gain deficits Δ_m and Δ_{-m} for the subthreshold modes. Lasing occurs near the frequency at which the maximum gain is achieved in the medium. Consider the case when the medium in which laser radiation propagates is 'perfect' (i.e., does not contain inhomogeneities). Then, the modal refractive index and the mode gain are the smooth functions of the frequency. The modal gain function near its maximum can be very accurately approximated by a second-degree polynomial. The gain deficit Δ of the subthreshold mode at the frequency ω is

$$\Delta(\omega) = \Delta(\omega_a) + \gamma(\omega - \omega_a)^2, \quad (20)$$

where ω_a is the position of the maximum of the mode gain curve and $g(\omega)$; $\gamma = -\frac{1}{2} \partial^2 g / \partial \omega^2$ is the parameter determining its curvature [the function $g(\omega)$ is determined in Appendix].

Taking into account that the gain deficit for the lasing mode should be zero and neglecting the non-equidistant location of the modes in this expression, we obtain the expression for parameters Δ_m and Δ_{-m} :

$$\Delta_{\pm m} = \Delta(\omega_0 \pm \Omega_m) = \pm \gamma \Omega_m (2\delta\omega \pm \Omega_m), \quad (21)$$

where $\delta\omega \equiv \omega_0 - \omega_a$ is the detuning of the lasing frequency from the maximum of the gain band. The quantities $\Delta_{\pm m}$ are explained qualitatively in the scheme in Fig. 1.

The parameter κ_m in the 'perfect' case under study has the form

$$\kappa_m = \frac{\Omega_m^2}{\tilde{n}_{\text{gr}}\omega_0} \left(\lambda^2 \frac{\partial^2 \tilde{n}}{\partial \lambda^2} \right). \quad (22)$$

Now we have all the initial data to find the effective gain deficits $\Delta_{\pm m}^{\text{eff}} = \Delta_{\pm m}^{\text{eff}}(\Omega_m, I, \delta\omega)$ and to analyse the stability of single-frequency lasing.

Consider first the case of low radiation intensities, when the terms proportional to χ_m in system (13) are small compared to Δ_m and Δ_{-m} . This takes place when $I \ll I_0$, where $I_0 = \alpha^{-1}(\Delta g/g_0)\Omega\tau I_{\text{sat}}$ (for $\alpha \gtrsim 1$) and $\Delta g = \gamma\Omega^2$ is the modal gain deficit for the first pair of modes at $\delta\omega = 0$, i.e., when the laser emission is exactly tuned to the spectral maximum of the material gain (here, Ω is the mode interval). The region of values of the variables Ω_m and $\delta\omega$ in this case is shown in Fig. 2a, where $\Delta_{\pm m}^{\text{eff}}(\Omega_m, I, \delta\omega) > 0$; the region is shaded and bounded by the beams $\delta\omega = \pm \Omega_m/2$. The solid horizontal segments show the intersections of the region with the straight lines $\Omega_m = m\Omega = m\pi c/(\tilde{n}_{\text{gr}}L)$, each of the segments determining the interval of values of $\delta\omega$ where the stability condition (17) is satisfied for the given m . The intersection of these intervals form the stability region for single-frequency lasing for the given intensity I . In the case

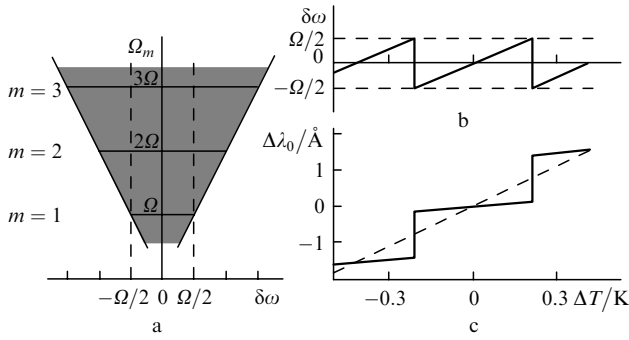


Figure 2. The case of low laser radiation intensities ($I \ll I_0$), when the interaction between the modes can be neglected: stable lasing region (a) and temperature dependences of the detuning $\delta\omega$ (b) and the lasing wavelength λ_0 (c).

under study ($I \ll I_0$), the stability region is the interval $(-\Omega/2; \Omega/2)$ whose width is equal to the mode interval. This is a simple and quite expected result, whose validity can be confirmed by Fig. 1 corresponding to a linear case.

Consider the process of continuous tuning of the lasing frequency ω_0 (or the laser wavelength λ_0) by varying temperature T under the conditions considered above. In principle, other external parameters, for example, pressure or the pump current can be used instead of temperature. We will assume that the lasing frequency $\omega_0(T_0)$ at temperature T_0 exactly coincides with the position ω_a of the gain maximum, i.e., $\delta\omega(T_0) = 0$ and the corresponding lasing wavelength is $\lambda_0 = 2\pi c/\omega_0$. We vary the temperature by δT near the point T_0 , which is located, for example, near 300 K. This leads to the temperature detuning $\delta\omega$ and the corresponding change in the lasing wavelength by $\delta\lambda_0 = \lambda_0(T_0 + \delta T) - \lambda_0(T_0)$.

The maximum ω_a of the gain band and longitudinal mode frequencies ω_m (including the lasing mode) shift with temperature at different rates ($\partial\omega_a/\partial T < \partial\omega_0/\partial T < 0$). Therefore, the detuning $\delta\omega$ also changes, and when it achieves the boundary of the stability region, lasing is switched to another mode. The lasing frequency ω_0 can be continuously tuned only when the detuning $\delta\omega$ remains within the stability region. The qualitative temperature dependence of the detuning $\delta\omega$ is shown in Fig. 2b. The calculated temperature dependence of the change $\delta\lambda_0$ in the lasing wavelength is shown in Fig. 2c. Hereafter, we use the following typical values of the laser parameters: $L = 1$ mm, $D = 3$ μm , $r_1 = 1$, $r_2 = 0.9$, $\lambda_0 = 0.98$ μm , $\tilde{n} = 3.4$, $\tilde{n}_{\text{gr}} = 3.7$, $\alpha = 3$, $\Delta g = 3 \times 10^{-3}$ cm^{-1} , $\lambda^2 \partial^2 \tilde{n} / \partial \lambda^2 = 2$, $\tau = 10^{-9}$ s, the diffusion length $A_D = \sqrt{\mu\tau} = 2.2$ μm , $\theta = 1$, $\partial\lambda_a/\partial T = 0.37$ nm K^{-1} , and $\partial\lambda_0/\partial T = 0.06$ nm K^{-1} .

Consider now the laser frequency tuning in the case $I \sim I_0$, i.e., when the nonlinear interaction of the modes becomes significant. For the values of the parameters presented above, we have $I_0 \approx 0.3I_{\text{sat}}$, which corresponds to the pump exceeding the lasing threshold by 30%. The stability region for single-frequency lasing found by the method described above is shown in Fig. 3a. A comparison of these data with the data presented in Fig. 2a shows that the stability region is shifted to the red and broadened. The temperature dependence of $\delta\omega$ is qualitatively shown in Fig. 3b, and the calculated temperature dependence of the lasing wavelength for this case is presented in Fig. 3c. The stability region of single-frequency lasing was $(-0.98\Omega; 0.23\Omega)$, i.e., its width is $\Delta\omega \approx 1.21\Omega$ for the above laser parameters.

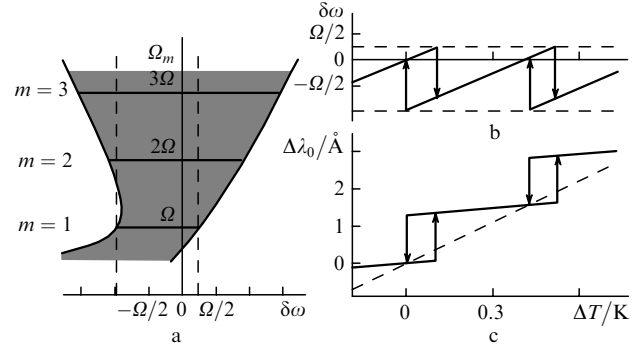


Figure 3. Behaviour of the laser system at the radiation intensity I of the order of the characteristic intensity I_0 (calculation was performed for $I = I_0$): stable lasing region (a) and temperature dependences of the detuning $\delta\omega$ (b) and the lasing wavelength λ_0 (c).

This new result follows exclusively from the nonlinear interaction of the modes and the deformation of the spectral contour of the effective gain due to parametric process via the carrier concentration oscillations at the intermode frequency. The increase in the detuning interval $\Delta\omega$, in which the mode switching is absent, with increasing the laser output power means an increase in the stability of single-frequency lasing, which can be called the self-stabilisation of the single-frequency regime. This was observed earlier in Refs [18, 19] for a laser with an external resonator. Some estimates of this effect were made in Ref. [19]. The increase in the tuning region $\Delta\omega$ can be treated qualitatively as additional absorption at optical frequencies nearest to the lasing mode induced by a 'strong' laser field (due to the parametric process). As a result, the influence of random fluctuations of the laser parameters (for example, temperature, pump current, and carrier concentration) on the mode switching can decrease with increasing laser power, i.e., the self-stabilisation of the single-frequency regime will occur.

Due to the expansion of the stability region, two modes can enter simultaneously this region at some temperatures, and single-frequency lasing can occur at any of these modes, i.e., bistable states appear. The lasing frequency in these states depends on the prehistory. In this case, the temperature dependence of the lasing frequency exhibits hysteresis loops, as shown in Figs. 3b, c.

Generally speaking, the radiation intensity also changes upon frequency tuning. However, these changes can be neglected upon the determination of the instant of mode switching (except the case of tuning by varying the pump current). As for the dependence of the radiation intensity on the tuning parameter, we note only that this dependence should also exhibit hysteresis when the width of the stability region exceeds the mode interval.

As the radiation intensity increases from zero to the value of the order of I_0 , the width of the stability region increases, resulting in the effects described above. As the radiation intensity I further increases, the dependence $\Delta\omega(I)$ becomes more complicated. This is explained by the fact that pairs of modes with $m > 1$ begin to affect the position of the stability region (see Fig. 4). The consideration of all the properties of the laser system at such intensities is beyond the scope of this paper. We mention here only two of them. First, breaks appear in the plot $\Delta\omega(I)$ of the dependence of the width of the stability region for the single-frequency regime on the radiation intensity (Fig. 5 shows

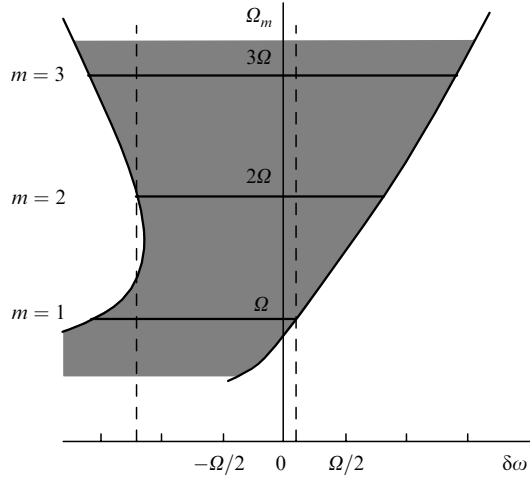


Figure 4. Stable lasing region at the radiation intensity I several times greater than the characteristic intensity I_0 , when the influence of the modes with $m > 1$ should be taken into account (calculation was performed for $I = 2I_0$).

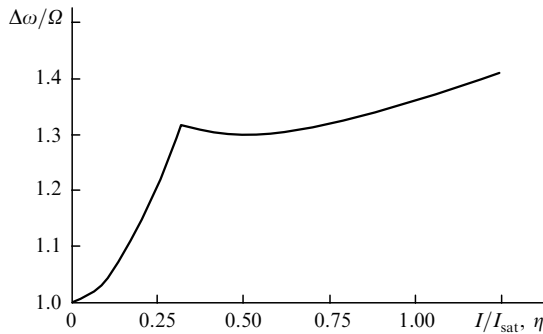


Figure 5. Dependence of the stability region width $\Delta\omega$ on the radiation intensity I and the relative excess of the pump over the threshold $\eta = J/J_{th} - 1$.

this dependence for the laser parameters presented above). Second, under some conditions, cascade mode switching appears, when, after the loss of the lasing stability at the initial mode, a mode located outside the stability region is first excited, and then lasing is switched to the mode located within this region.

4. Discussion and conclusions

We have shown for the first time that in a semiconductor laser with a Fabry–Perot resonator formed by laser's own facets and a homogeneous active medium, the self-stabilisation of single-frequency lasing regime can occur. As a result, a continuous tuning of the laser frequency can be performed within the interval of detuning from the spectral maximum of the material gain exceeding the mode interval. In this case, the single-frequency regime can exhibit an increased stability with respect to the mode switching, and a spectrally bistable lasing regime can be observed.

Such behaviour is explained by the parametric process caused by optical nonlinearity, resulting in the coupling between the spectral amplitudes of the fields. We have considered here the most general case of three optical frequencies, with the field amplitude at the central frequency

being greater than the amplitudes at two other frequencies corresponding to the red and blue components. In the presence of only two fields, one of them weak and another strong, which corresponds, for example, to the case when the field of one of the components is suppressed, this process can be treated as stimulated scattering from the electron density, as was first performed in Ref. [7]. In the case of two fields, the nonlinear interaction of the fields is spectrally asymmetric. The strong field induces additional gain in the Stokes region of the spectrum and absorption in the anti-Stokes region. Of course, the interaction of this type is only a particular case of the theory presented here.

This theory does not use any physical parameters whose values would be difficult to measure in independent experiments. The parametric coupling between the field amplitudes via the population inversion is a fundamental property of a laser system and of the saturation gain effect, so that its presence in a physical model analysing the spectrum is a natural and necessary factor.

Note in this connection a number of papers (see, for example, Refs [20, 21]) in which was stated without proof that, because the beat frequency Ω is high compared to the inverse interband relaxation time $(\tau_{eff})^{-1}$, the interaction between the modes caused by oscillations of the total carrier concentration in bands does not play any role due to a small amplitude of these oscillations. The authors of these papers considered for this reason instead of interband relaxation of carriers only their intraband relaxation. The intraband relaxation time τ_i is substantially shorter, so that $\Omega \ll (\tau_i)^{-1}$, and therefore, this relaxation mechanism dominates in the opinion of authors [20, 21]. We believe that such reasoning is groundless because it is exclusively intuitive and is not verified quantitatively, as was done in our paper. A shortening of the relaxation time reduces the response amplitude simultaneously at all the frequencies, the time shortening being strongest at lower frequencies, resulting in the blue shift of the spectral response. This circumstance is a basic property of the relaxation system, which is related to the population inversion or carrier concentration. In other words, we can consider some subsystem within the electronic system, which is located in the energy band corresponding to the homogeneous width. Carriers in such subsystem can interact with a laser field, and they are connected with the remaining system by a shorter intraband relaxation time. In our opinion, the quantitative result of such an approach will not differ substantially from the result obtained in our paper, but is more difficult to obtain.

Another consideration, which allows us to ignore intraband relaxation, is that it is difficult to expect the deviation of the carrier density distribution from the Fermi function because the Coulomb interaction between carriers forming this distribution is simultaneously strong and long-range. In our opinion, there is no conclusive experimental evidence of the possibility of such deviations at the time scale considered. Of all the processes of the intraband relaxation of carriers, which can really take place, we ignored in this paper only one – ‘the detachment’ of the temperature of carriers with the Fermi distribution from the crystal lattice temperature. This process proceeds slower than the establishment of the Fermi distribution, and its characteristic time can be $\sim 10^{-13}$ s.

The interaction of the fields, taking into account this mechanism, was considered in Ref. [22], where it was shown

that this mechanism introduces only some quantitative correction. This corresponds to the above conclusion that a decrease in the relaxation time of the system (subsystem) does not enhance its response. By concluding the discussion of the influence of the beats of the total carrier concentration on the interaction between longitudinal modes, we point out paper [23] in which these beats were directly observed. Concerning a comparison of our theory with experiments, we note that one of the manifestations of self-stabilisation is the presence of a hysteresis loop in the temperature dependence of the wavelength or the pump current. Although this was earlier observed in many experiments (see, for example, Ref. [24]), and the characteristic parameters of the spectral bistability region are quantitatively close to the calculated values (see, for example, Fig. 3), further experiments are required to confirm a complete coincidence between the theory and experiment. To provide an adequate comparison of the theory with experiment, it is necessary to have high-quality samples with high optical homogeneity along the resonator axis, thereby ensuring the absence of a random uncontrollable selectivity.

Note in conclusion that the results presented in Figs 2–5, which were obtained for certain laser parameters, are of a quite general type. We have found that the variation in the laser parameters causes only some quantitative changes in the results, retaining their qualitative behaviour invariable.

Acknowledgements. The authors thank A.E. Drakin for useful discussions and his help in the study. This work was supported by the Federal Scientific and Technological Programs ‘Quantum and Nonlinear Processes’ and ‘Physics of Solid Nanostructures’, the ‘Integration’ Program (project ‘Fundamental Optics of Quantum-Well Semiconductors’), and partially supported by a grant of the ‘Leading Scientific Schools’ (No. 00-15-96624).

Appendix

Derivation of the system of equations for the complex amplitudes of the modes

The transverse distribution of the field $u(x, y)$ in the resonator and the mode (effective) permittivity $\tilde{\epsilon}(\omega, N)$ are found as the eigenfunction and the eigenvalue of the equation

$$\left(\frac{\partial^2}{\partial x^2} + \frac{\partial^2}{\partial y^2} \right) u(x, y) + \frac{\omega^2}{c^2} [\epsilon(x, y, \omega, N) - \tilde{\epsilon}(\omega, N)] u(x, y) = 0 \quad (\text{A1})$$

with the boundary conditions at the laser facets. The solution of equation (A1) is a separate problem, which can be solved, for example, by the method described in Ref. [17].

The mode gain $g(\omega, N)$ can be expressed in terms of the effective permittivity in a standard way as $g(\omega, N) = -(2\omega/c) \text{Im}[\tilde{\epsilon}(\omega, N)]^{1/2}$, and the effective refractive index \tilde{n} is $\tilde{n} = \text{Re}[\tilde{\epsilon}(\omega, N)]^{1/2}$.

Function (2) is the solution of the wave equation (1) under the condition

$$\beta_0^2 = \left(\frac{\omega_0}{c} \right)^2 \tilde{\epsilon}(\omega_0, N_0), \quad (\text{A2})$$

which, together with conditions (3) and (4), and equation (10), determines the laser mode frequency and the threshold carrier concentration N_0 .

By substituting expression (5) for the field into the wave equation (1), taking into account (23) and the expression $V_m(z) = r_1 e^{i\beta_m z} + e^{-i\beta_m z}$, where $\beta_m = \beta_0 + \pi m/L$, we obtain the system of equations for the complex amplitudes of the modes

$$\frac{1}{2} \left\{ \frac{2i\omega_m \tilde{n}_m \tilde{n}_{\text{gr}m}}{c^2} \dot{C}_m(t) + \left[\frac{\omega_m^2}{c^2} \tilde{\epsilon}(\omega_m) - \beta_m^2 \right] C_m(t) \right\} V_m(z) \times u(x, y) - \frac{1}{c^2} e^{i\omega_m t} (\alpha + i) \frac{d\epsilon''}{dN} \frac{\partial^2}{\partial t^2} [\delta N(\mathbf{r}, t) E_0(\mathbf{r}, t)]_{\omega_m} = 0, \quad (\text{A3})$$

where $\tilde{n}_m \equiv [\tilde{\epsilon}(\omega_m)]^{1/2}$; $\tilde{n}_{\text{gr}m} \equiv [\tilde{n} + (\partial\tilde{n}/\partial\omega)\omega]_{\omega_m}$; and $\alpha = (d\epsilon'/dN)(d\epsilon''/dN)^{-1}$; $[\delta N(\mathbf{r}, t) E_0(\mathbf{r}, t)]_{\omega_m}$ is the component of this expression at frequencies near ω_m .

The representation of the field in form (5) gives formally a certain arbitrariness in the choice of frequencies ω_m , which is restricted only by the requirement that the amplitude $C_m(t)$ should be ‘slow’. The mode interval $\omega_m - \omega_{m-1}$ changes weakly with m (compared to the interval $\omega_m - \omega_{m-1}$ itself), so that we can assume for $m > 0$ that

$$\omega_m = \omega_0 + \Omega_m,$$

$$\omega_{-m} = \omega_0 - \Omega_m,$$

by determining Ω_m from the condition

$$\frac{\omega_m^2}{c^2} \tilde{\epsilon}(\omega_m) - \beta_m^2 = \frac{\omega_m \tilde{n}_m}{c} i\Delta_m, \quad (\text{A4})$$

where Δ_m is a real quantity. This equation also determines the mode gain for the m th mode. For the $-m$ th mode, we can write

$$\frac{\omega_{-m}^2}{c^2} \tilde{\epsilon}(\omega_{-m}) - \beta_{-m}^2 = \frac{\omega_{-m} \tilde{n}_{-m}}{c} \left(\frac{2\tilde{n}_{\text{gr}(-m)}}{c} \kappa_m + i\Delta_{-m} \right), \quad (\text{A5})$$

where Δ_{-m} and κ_{-m} are also real quantities.

The quantities Δ_m , Δ_{-m} and κ_m introduced this way coincide with the mode gain deficits and the frequency asymmetry in the location of the modes with respect to the lasing mode, respectively. They characterise the spectral properties of the active medium, including its dispersion, and of the resonator at the lasing threshold, i.e., they are the parameters of the laser as a linear system. This is confirmed by the form of equations obtained for the mode amplitudes.

For the complex frequencies ω'_m of the subthreshold modes at the lasing threshold, we have

$$\omega'_m = \omega_m + \Omega_m - i(c/2\tilde{n}_{\text{gr}})\Delta_m$$

$$\text{for the blue spectral region} \quad (\text{A6a})$$

and

$$\omega'_{-m} = \omega_0 - \Omega_m - \kappa_m - i(c/2\tilde{n}_{\text{gr}})\Delta_{-m}$$

$$\text{for the red spectral region.} \quad (\text{A6b})$$

The positions of the modes and their gain deficits at the lasing threshold are shown schematically in Fig. 1.

By neglecting the dependence of the coefficient at $\dot{C}_m(t)$ on m in equation (25), multiplying it by $V_m(z)u(x, y)$, and integrating over the resonator volume, we obtain, using (12), (26), and (27), the system (13) with the coefficients A_m and B_m described by the expressions

$$A_m = \frac{8i\pi\hbar\omega_0(\omega_m - \omega_0) \int V_0(z)V_m(z)[u(x, y)]^2 f_m^*(\mathbf{r})dV}{G_0cn \int [V_m(z)u(x, y)]^2 dV}, \quad (\text{A7})$$

$$B_m = \frac{8i\pi\hbar\omega_0(\omega_m - \omega_0) \int V_0(z)V_m(z)[u(x, y)]^2 f_{-m}(\mathbf{r})dV}{G_0cn \int [V_m(z)u(x, y)]^2 dV},$$

where n and G_0 are the refractive index and the characteristic value of the gain in the active region; integration here is performed over the active region.

References

1. Bachert H., Bogatov A.P., Eliseev P.G., Keiper A., Khairetdinov K.A. *IEEE J. Quantum Electron.*, **15** (8), 786 (1979).
- [doi>](#) 2. Ruhle W., Brosson P. *J. Appl. Phys.*, **51** (11), 5949 (1980).
- [doi>](#) 3. Mukai T., Inoue K., Saitoh T. *Appl. Phys. Lett.*, **51** (6), 381 (1987).
4. Lamb W., in *Quantum Optics and Electronics* (Les Houches Summer School Lectures) (New York: Gordon and Breach, 1964; Moscow: Mir, 1966) p.315.
5. Belenov E.M., Morozov V.N., Oraevsky A.N. *Trudy FIAN*, **52**, 237 (1970).
6. Kuznetsova T.I. *Trudy FIAN*, **43**, 116 (1968).
7. Bogatov A.P., Eliseev P.G., Sverdlov B.N. *IEEE J. Quantum Electron.*, **11** (7), 510 (1975).
8. Agrawal G.P. *Opt. Lett.*, **12** (4), 260 (1987).
9. Ogasawara N., Ito R. *Jpn. J. Appl. Phys.*, **27** (4), 615 (1988).
- [doi>](#) 10. Mukai T., Saitoh T. *IEEE J. Quantum Electron.*, **26** (5), 865 (1990).
11. Bogatov A.P., Eliseev P.G., Kobildzhanov O.A., Madgazin V.R. *IEEE J. Quantum Electron.*, **23** (6), 1064 (1987).
12. Bogatov A.P., Rakhval'skii M.P. *Laser Phys.*, **2** (4), 533 (1992).
13. Bogatov A.P. *J. Russian Laser Research*, **15** (5), 417 (1994).
14. Bezotosnyi V.V., Bogatov A.P., Dolginov L.M., Drakin A.E., Eliseev P.G., Mil'vidskii M.G., Sverdlov B.N., Shevchenko E.G. *Trudy FIAN*, **141**, 18 (1983).
15. Hayward J.E., Cassidy D.T. *J. Opt. Soc. Am. B*, **9** (7), 1151 (1992).
- [doi>](#) 16. Hofstetter D., Thornton R.L. *IEEE J. of Quantum Electron.*, **34** (10), 1914 (1998).
- [doi>](#) 17. Klehr A., Beister G., Erbert G., Klein A., Maeger J., Rechenberg I., Sebastian J., Wenzel H., Tränkle G. *J. Appl. Phys.*, **90** (1), 43 (2001).
18. Akul'shin A.M., Bazhenov V.Yu., Velichaskii V.L., Zverkov M.V., Zibrov A.S., Nikitin V.V., Okhotnikov O.G., Sautenkov V.A., Senkov N.V., Yurkin E.K. *Kvantovaya Elektron.*, **13**, 1391 (1986) [*Sov. J. Quantum Electron.*, **16**, 912 (1986)].
19. Bogatov A.P., Eliseev P.G., Okhotnikov O.G., Rakhval'skii M.P., Khairetdinov K.A. *Kvantovaya Elektron.*, **10**, 1851 (1983) [*Sov. J. Quantum Electron.*, **13**, 1221 (1983)].
- [doi>](#) 20. Kazarinov R.F., Henry C.H., Logan R.A. *J. Appl. Phys.*, **53**, 4631 (1982).
21. Agrawal G.P. *Appl. Phys. Lett.*, **51**, 303 (1987).
- [doi>](#) 22. Plyavenek A.G. *Opt. Commun.*, **100**, 278 (1993).
- [doi>](#) 23. Sharfin W.F., Schlafer J., Koteles E.S. *IEEE J. Quantum Electron.*, **30** (8), 1709 (1994).
24. Garrett B., White I.H., Gallagher D.F.G. *Electron. Lett.*, **23**, 1193 (1987).